Apparent Inverse Gibbs-Thomson Effect in Dealloyed Nanoporous Nanoparticles

I. McCue, J. Snyder, X. Li, Q. Chen, K. Sieradzki, and J. Erlebacher

Phys. Rev. Lett. **108**, 225503 — Published 31 May 2012

DOI: 10.1103/PhysRevLett.108.225503

An Apparent Inverse Gibbs-Thomson Effect in Dealloyed Nanoporous Nanoparticles

I. McCue[1], J. Snyder[1], X. Li[2], Q. Chen[2], K. Sieradzki[2], J. Erlebacher*[1]

[1]Department of Materials Science and Engineering, Johns Hopkins University, Baltimore, MD 21218

[2]Materials Science and Engineering, Arizona State University, Tempe, AZ 85287-6106

Abstract

The Gibbs-Thomson effect (the reduction of local chemical potential due to nanoscale curvature) predicts that nanoparticles of radius r dissolve at lower electrochemical potentials than bulk materials, decreasing as $1/r$. However, we show here that if the particle is an alloy – susceptible to selective dissolution (dealloying) and nanoporosity evolution – then complete selective electrochemical dissolution and porosity evolution requires a *higher* electrochemical potential than the comparable bulk planar material, increasing empirically as $1/r$. This is a kinetic effect, which we demonstrate via kinetic Monte Carlo (KMC) simulation. Our model shows that in the initial stages of dissolution, the less noble particle component is easily stripped from the nanoparticle surface, but owing to an increased mobility of the more noble atoms, the surface of the particle quickly passivates. At a fixed electrochemical potential, porosity and complete dealloying can only evolve if fluctuations in the surface passivation layer are sufficiently long-lived to allow dissolution from percolating networks of the less-noble component that penetrate through the bulk of the particle.

Dealloying refers to the selective electrochemical dissolution of one or more components from an alloy, leaving behind a material enriched in the more-noble alloy component [1,2]. Under conditions where the dissolution rate is fast enough relative to the surface diffusion rate of the undissolved component, it is well-established that a nanoscale pattern forming instability arises that drives the formation of nanoporosity during dealloying of bulk alloys, with ligament and pore sizes in some cases less than 5 nm [3]. Historically, dealloying has been studied in the context of corrosion, but has received renewed recent attention due its re-invention as a nanoscale processing tool to fabricate ultra-high surface area materials for catalysis, sensing, and optical applications [4,5,6]. Dealloyed nanoparticles are potentially excellent electrocatalysts, combining the high surface area/volume features of traditional nanoparticles with the ability to tune composition and morphology for improved functionality [7,8]. Typically this is accomplished by electrochemical potential cycling between prescribed voltage limits, sometimes yielding a variety of dealloyed nanoparticle types including core-shell and nanoporous structures. Nanoporous particles are of additional interest because the porous region can be filled with secondary phases to form nanoreactors [9], and offer a platform on which to study nanoscale surface diffusion dynamics on high-curvature crystal surfaces [10]. Nanoporous metals generally exhibit unusual physical behavior associated with their structure including nanoscale manifestations of thermodynamic surface stress [11] and high magnetoresistance [12].

Thermodynamically, dealloying is favorable above a particular critical electrochemical potential E_{crit} that balances the free energy reduction associated with dissolution into solution with the energetic penalty associated with any new roughness and surface area created [2]. The energy gain associated with electrochemical dissolution is a strong function of the curvature of the surface, and for single component materials the electrochemical potential decreases with

particle radius r as a function of $1/r$ due to the Gibbs-Thomson effect [13,14]. It might be expected that the potential at which porosity forms in a nanoparticle should also decrease with decreasing radii, but here we report the results of kinetic Monte Carlo simulations (KMC) showing that this potential actually *increases* with $1/r$ in alloy nanoparticles. The origin of this effect lies in the details of nanoparticle alloy dissolution – generally, regardless of potential, dealloying nanoparticles initially and quickly tends to form noble-metal passivated particles. Porosity only forms over longer timescales if the dissolution rate is high enough to form pits during transient surface fluctuations that expose less-noble atoms buried under step edges to the external environment. Such surface fluctuations increase in frequency but decrease in duration with smaller particle size because of the rise in surface mobility associated with the Gibbs-Thomson effect (such fluctuations can be considered the initial manifestation of the melting point suppression in nanoparticles).

To study selective dissolution in alloy nanoparticles, we used the KMC simulation code MESOSIM, a full description of which can be found in Ref. [15]. Briefly, MESOSIM has been optimized to reflect time and energy scales associated with the prototypical Ag-Au dealloying system (in which silver dissolution competes with surface diffusion of gold, leading to nanoporous gold), but the general trends here should be applicable to dealloyable systems that remain single phase. Simulations are initialized by placing atoms on a 3-dimensional fcc lattice and the type of atom (Ag or Au) is assigned at random based on a weighted probability determined by the composition of the alloy. The time evolution of the system is governed by the KMC algorithm. In KMC, if there are N total events that can occur, each one indexed by i and possessing rate k_i, the time for a single event to occur is $\Delta t = -\ln \xi \Big/ \sum_{i=1}^{N} k_i$ where ξ is a random

number in (0,1]. Within this time the probability of an event occurring is $P_i = k_i \Big/ \sum_{j=1}^{N} k_j$. KMC simulations progress by picking a random event according to its weighted probability (more unstable events are weighted heavier than stable ones) and then the time is incremented accordingly. Our model here is a draws on the model introduced in Ref [16] and uses a simple bond-breaking model to capture the generic morphological evolution physics occurring over experimental timescales. Specifically, rates for surface diffusion (of both silver and gold) and dissolution (of only silver) at an electrochemical potential ϕ are given by the expressions $k_{diff} = v_1 \exp\left[-\frac{nE_B}{k_b T}\right]$, and $k_{diss} = v_2 \exp\left[-\frac{nE_B - \phi}{k_b T}\right]$, where $v_1 = 10^{13}\,\text{sec}^{-1}$, $v_2 = 10^{4}\,\text{sec}^{-1}$, $E_B = 0.15\,\text{eV}$ for all bond energies, and n is the number of bonds in the initial state. The parameters and kinetic expressions have been shown in other studies to accurately model dissolution current versus potential behavior [1,15,15,17]; the parameters also successfully model coarsening in nanoporous nanoparticles [10] that agree with timescales of experimental studies of coarsening of nanoporous gold (which we note are generally much longer than any of the timescales discussed in this work)[18]; and recently an experimental measurement of the activation barrier for dissolution of Ag from a terrace site of a Ag/Au alloy was measured and found to be consistent with a bond energy between 0.1-0.2 eV [19].

Figure 1 shows a representative time evolution of a simulated nanoparticle of radius 30 and composition 75 at. % Ag. Overall, three different compositions were examined: 65, 75, and 85 at. % Ag; and four different nanoparticle radii: 8, 11, 18, 30 ± 1 atom diameters. These values approximately correspond to nanoparticle diameters of ~4, 6, 10, and 17 nm. The compositions were chosen to be representative of the composition range typically found in porosity-forming dealloying systems [15]. Smaller particles were not studied because the

roughness that evolved in the initial stages of dissolution was greater in amplitude than the particle diameter, and porosity never evolved. Particles were dealloyed under constant potential at 300 K and ran between 10^4-10^5 simulated seconds or ~$5x10^8$ iterations. The behavior exemplified by the particle in Figure 1 shows the following characteristics: (a) at short times, $t < 10^2$ sec., the outmost silver atoms are quickly stripped. Unlike the case of a bulk, planar surface, there are always low-coordination Ag atoms sitting at step edges at facet boundaries that facilitate such stripping; (b) at intermediate times $t < 10^3$ sec. , the particle is passivated with a monolayer of gold, which surface diffuses, pushing the shape of the particle toward the-equilibrium Wulff shape (if we start the simulations with particle shapes already equilibrated to the Wulff shape rather than a sphere, our results are unchanged); (c) over long time periods, regions of the bulk are exposed to the external environment due to fluctuations in the outermost layer; (d) in some cases, these fluctuations are long-lived enough to allow further attack into the interior of the nanoparticle. An important point here is that fluctuations exposing the interior also appear in stage (a), but the concurrent dissolution of the outermost silver is roughening the surface so quickly that there are always nearby gold atoms that can diffuse into terrace vacancies resulting in transient passivation.

In dealloying of bulk planar materials, the critical potential is a sharp threshold separating porosity formation from surface passivation [20]. Analogously in nanoparticles, we find an increase in the propensity for porosity evolution to exist as the electrochemical potential increases, but this threshold is not sharp. To quantify this observation, for each particular radius and electrochemical potential we generated a histogram over the course of many runs (Figure 2), typically many thousand, showing the final volume of the particle after being subjected to a dissolution potential for some fixed, but long, period of time (10^4 sec). Near a potential for

porosity evolution E_P, distinct from and larger than the critical potential for the bulk planar alloy, we see two Gaussian distributions corresponding to two final particle volumes. The distribution at smaller volume corresponds to fully dealloyed and porous particles that have lost the majority of their less-noble component mass, and the other corresponds to particles that have undergone only superficial surface dealloying and become passivated with the noble component. For this latter case, there is still a significant amount of the less noble component buried in the particle. We define E_P as that potential where the area of each Gaussian distribution is equal. We note that by the particular time at which the mass distribution was assessed (10^4 sec.), the distribution had reached a steady state; that is, we occasionally checked that non-porous particles subjected to the potential E_P over a time 10^4 do not dissolve further even if the simulations are run for an order of magnitude in time longer.

Figure 3 shows E_P for the three compositions plotted against the inverse particle radius. For reference, bulk values for the critical potential reported in Ref. [15] are plotted at $1/r = 0$. Most notably, the potential associated with porosity evolution E_P is seen to *increase* as the particle size decreases. This observation should not be interpreted to mean that it is more difficult energetically to dissolve silver atoms from smaller particles than from larger ones. All the particles here quickly lose silver from their initial surface, and, in accordance with the Gibbs-Thomson effect, at fixed potential smaller particles tend to lose their surface silver more quickly because they have a higher fraction of low-coordinated step and kink sites [13]. However, for the same reason, the gold atoms left behind on the alloy particle surface are much more mobile on the smaller particles and thus quickly passivate the interior. It is possible that reduction of the

ratio k_{diff}/k_{diss} could reduce such passivation at a fixed particle size and potential, but it is unclear how to experimentally achieve this.

We necessarily conclude that E_P is fundamentally kinetic in origin, containing a complex choreography of surface composition fluctuations convoluted with the geometric connectivity of the more reactive component under the passivating gold surface. The ingredients that need to be included in a kinetic model for E_P include:

(i) An observation that the initial stage of porosity evolution in particles must be gold-passivated particles and not a surface with an appreciable concentration of silver. After this initial stage, there are a few silver atoms exposed on the surface on the low-index facets, but the majority of silver atoms still on the surface sit along facet boundaries in 10- and 11-coordinated sites (see, for instance, the third image in Figure 1). For this reason, the number of exposed silver atoms at this stage of evolution increases approximately linearly with the particle radius.

(ii) The majority of surface diffusion events that can lead to further exposure of silver to the electrolyte, or reduction of silver coordination, are fluctuations at step edges that reduce the coordination of 10- and 11-coordinated silver atoms to 9-coordinated terrace sites susceptible to attack by electrolyte. Over long periods of simulated time, of order 10^4 sec, many Ag atoms are transiently exposed to the electrolyte. The 9- coordination number corresponds geometrically to a terrace atom in a (111)-oriented surface, and it has been shown that this is likely the maximum coordination for which dissolution occurs [19,21]; physically, more highly coordinated atoms are thought not to be sterically complexable by anions in solution. Within the model, the lifetime of the fluctuation exposing Ag atoms is independent of the dissolution potential. At the very least, for porosity to form, this lifetime must be larger than the average time to dissolve silver from such a terrace site.

(iii) Finally, assuming the Ag atom is dissolved within the lifetime of a surface fluctuation, porosity can form only if the surface Ag atom is connected to a percolation network of other Ag atoms through the bulk of the particle. In contrast to the early stages of dissolution, where there are many Au atoms diffusing on the surface that are readily available to passivate low-coordinate surface defects, the surface vacancies associated with dissolution of silver atoms during these surface fluctuations are very long-lived. As a result, we observe that if a percolation network of silver atoms starts to dissolve after the particle has reached the pseudo-equilibrated Wulff shape, the entire particle will almost instantaneously dealloy and become porous.

Taken together, these observations lead to a first order master equation describing the rate of change of the number of exposed 9-coordinated silver atoms N_{Ag}:

$$\frac{dN_{\mathrm{Ag}}}{dt} = -k_{diss} P_{kink} P_{perc} N_{\mathrm{Ag}} \qquad (1)$$

Here, k_{diss} is the dissolution frequency from a 9-coordinated site, P_{kink} is the probability a kink site has fluctuated with large-enough amplitude to expose a silver atom, and P_{perc} is the probability this silver atom is connected to a percolation network into the bulk. Because a single dissolution event at this stage tends to lead to porosity evolution, the simplest criterion for E_P is determined by the condition that over a period of time Δt equal to the lifetime of the step edge fluctuation the number of surface silver atoms decreases by one: $N_{Ag}(\Delta t) \le N_{Ag}(0) - 1$. Solving Eq. (1) under this condition and noting that the simulation rule $k_{diss} = \nu \exp\left[-\left(9E_B - E_P\right)/k_B T\right]$, we find E_P is determined by

$$E_P \geq 9E_B + k_b T \ln\left[\frac{-1}{\nu P_{kink} P_{perc} \Delta t} \ln\left(\frac{N_{Ag}(0)-1}{N_{Ag}(0)}\right)\right] \quad (2)$$

The simulation model allows P_{perc}, $N_{Ag}(0)$, P_{kink} and Δt to be quantitatively measured independently. For percolation and $N_{Ag}(0)$, particle dissolution was halted upon completion of the passivation layer, and 9-coordinated silver atoms were counted and checked to see whether or not they belonged to a percolation network. A high-density percolation (HDP) threshold criterion was used to determine if a silver atom belonged to a percolation network, following Ref. [21], requiring Ag atoms to be counted in the percolating network if at least nine of its twelve potential neighbors are also silver. As discussed in Ref. [21], this criterion is equivalent to the physically reasonable requirement that there be enough free volume around a surface silver atom for it to be solvated and dissolved by the electrolyte. Not surprisingly over the particle sizes examined, we find little size dependence of the probability of belonging to such a percolation network, with the probabilities equaling ~42%, ~81%, and ~97%, for compositions of 65, 75 and 85 at. % Ag. For $N_{Ag}(0)$, we find a weak linear dependence (see inset of Figure 3) on the particle radius, reflecting how most of the exposed 9-coordinated silver atoms appear due to fluctuations exposing 10- and 11-coordinated atoms that sit on facet boundary regions , the length of which increases linearly with particle radius.

The largest particle size-dependence is found for P_{kink} and Δt , the measures associated with fluctuations that lead to transient exposure buried of surface silver atoms. To quantify this effect, gold-passivated particles were again generated, but then silver atoms were not allowed to dissolve or diffuse during the further course of the simulation. These simulations tracked the time interval between a silver atom becoming 9-coordinated, and then becoming buried (i.e., re-

passivated) by surface diffusing gold. Histograms of these time intervals for radius 8 and radius 30 particles are shown in Figure 4, and exhibit a rich complexity. For both particle sizes shown, we see that the majority of fluctuations are short-lived – 10^{-6} to 10^{-7} sec. – with a slight shift as the size increases to radius 30. These fluctuations are associated with gold adatoms moving over silver atoms embedded in terraces. Longer-lived fluctuations are associated with surface diffusion of gold with increasing coordination, so, for instance, the peak centered around 1 to 10 seconds corresponds to particular fluctuations of interest involving atoms at kink sites that expose 9-coordinated silver atoms. The difference in frequency distribution with particle size is straightforwardly explained as a Gibbs-Thomson effect: Surfaces on the $r = 8$ particles are extremely unstable and Ag terrace passivation is controlled by adatom events, but as the radius increases the concentration of highly mobile low-coordination surface atoms decreases and a majority of the passivation events become controlled by lower-coordination surface atoms participating in attachment/detachment events at kink sites. As the longer-lived fluctuations are the ones that ultimately lead to porosity evolution, we associate P_{kink} and Δt with the longer-lived kink-site fluctuations, P_{kink} being the area under the peak associated with Δt_{kink}.

Using the independently measured values for the time interval, percolation and kink probabilities, and terrace concentration data into Eq. (2) we find good agreement with the model and the measured values of E_P (see Figure 3). The slopes for both the simulation and analytical models for 65 and 75 at.% Ag are approximately the same, but the slope for the 85 at. % simulation data is steeper than that predicted by Eq. (2). We resolve this discrepancy by noting that at high silver fractions, the pseudo-Wulff particle has approximately 15% of its surface silver atoms on (001) facets, in addition to the majority (111) positions. This means the average activation barrier for dissolution in this case is slightly smaller than $9E_b - E_P$. In fact, we find

good agreement between model and simulation using $8.9E_b - E_P$ in Eq. (2) at the 85 at. % composition, as shown in Figure 3. .

The work presented here impacts tuning the composition and morphology of dealloyed nanoparticles in the following ways. First, it may require surprisingly high electrochemical potentials to both fully dealloy a nanoparticle and ensure that every particle in a batch is porous. In experiments, this is often accomplished by electrochemical cycling which has the effect of "artificially" increasing the magnitude, lifetime and frequency of surface compositional fluctuations. Second, the work here suggests that stymieing the surface mobility of the more noble (passivating) component can lead to more facile porosity evolution in nanoparticles, perhaps by adsorbing a self-assembled monolayer or dealloying under conditions where this component forms a stable oxide [22,23].

To summarize, the size dependence of surface site duration, percolation probability, and concentration of surface sites has been examined for binary alloy fcc nanoparticles. A first order rate equation provides a reasonable explanation of the increase in the electrochemical potential necessary for porosity evolution, and we identify the primary source of the increase to be a Gibbs-Thomson effect acting upon the gold-passivation layer on the particle. While for small particles there are many small fluctuations in the surface morphology, these fluctuations are too short-lived to lead to further dissolution. Porosity evolution occurs when fluctuations are long-enough lived to allow silver dissolution, and surface fluctuation lifetime increases with particle radius.

Acknowledgements

JE and KS are grateful to the NSF for financial support under programs DMR-1003901 and DMR-0855969.

References

[1] J. Erlebacher *et al.*, *Nature (London)* **410**, 450 (2001).

[2] J. Rugolo, J Erlebacher, and K. Sieradzki, *Nature Mater*. **5**, 946 (2006).

[3] J. Erlebacher *et al.*, *MRS Bull.* **34**, 561 (2009).

[4] Y. Ding, M.W. Chen, and J. Erlebacher, *J. Am. Chem. Soc.* **126**, 6876 (2004).

[5] M. Heida, *Appl. Phys. Lett.* 84, 628 (2004).

[6] Kramer, R.N Viswanath, and J. Weissmuller, *Nano Lett.* **4**, 793 (2004).

[7] D. Wang, P. Zhao, and Y. Li, *Sci. Rep.* **1:37** (2011).

[8] M. Shao *et al.*, *J. Am. Chem. Soc.* **132,** 9253 (2010).

[9] J. Snyder, T. Fujita, M.W. Chen, J. Erlebacher, *Nature Mater.* **9**, 904 (2010).

[10] J. Erlebacher, Phys. Rev. Lett. **106**, 225504 (2011)

[11] S. Parida *et al.*, Phys. Rev. Lett. **97**, 035504 (2006)

[12] T. Fujita *et al.*, Phys. Rev. Lett. **101**, 166601 (2008)

[13] L. Tang et al. *J. Electrochem. Soc.* **132**, 596 (2010).

[14] E.F. Holby *et al.*, *Energy Environ.* Sci. **2**, 865 (2009).

[15] J. Erlebacher, *J. Electrochem. Soc.* **151**, C614 (2004).

[16] N. Combe, P. Jensen, A. Pimpinelli, Phys. Rev. Lett. **85**, 110 (2000)

[17] S.A. Policastro et al., *J. Electrochem. Soc.***157**, C328 (2010)

[18] Y. Ding, Y. Kim, J. Erlebacher, *Adv. Mater.* **16**, 1897 (2004)

[19] J. Snyder and J. Erlebacher, *J. Electrochem. Soc.* **157**, C125 (2010).

[20] K. Sieradzki *et al.*, *J. Electrochem. Soc.* **149**, B370 (2002).

[21] D.M. Artymowicz, J. Erlebacher, and R.C. Newman, *Philo. Mag.* **89**, 1663 (2009).

[22] T.P. Moffat, F.F. Fan, and A.J Bard, *J. Electrochem. Soc.* **138**, 3224 (1991).

[23] J. Snyder, K. Livi, and J. Erlebacher, *J. Electrochem. Soc.* **155**, C464 (2008).

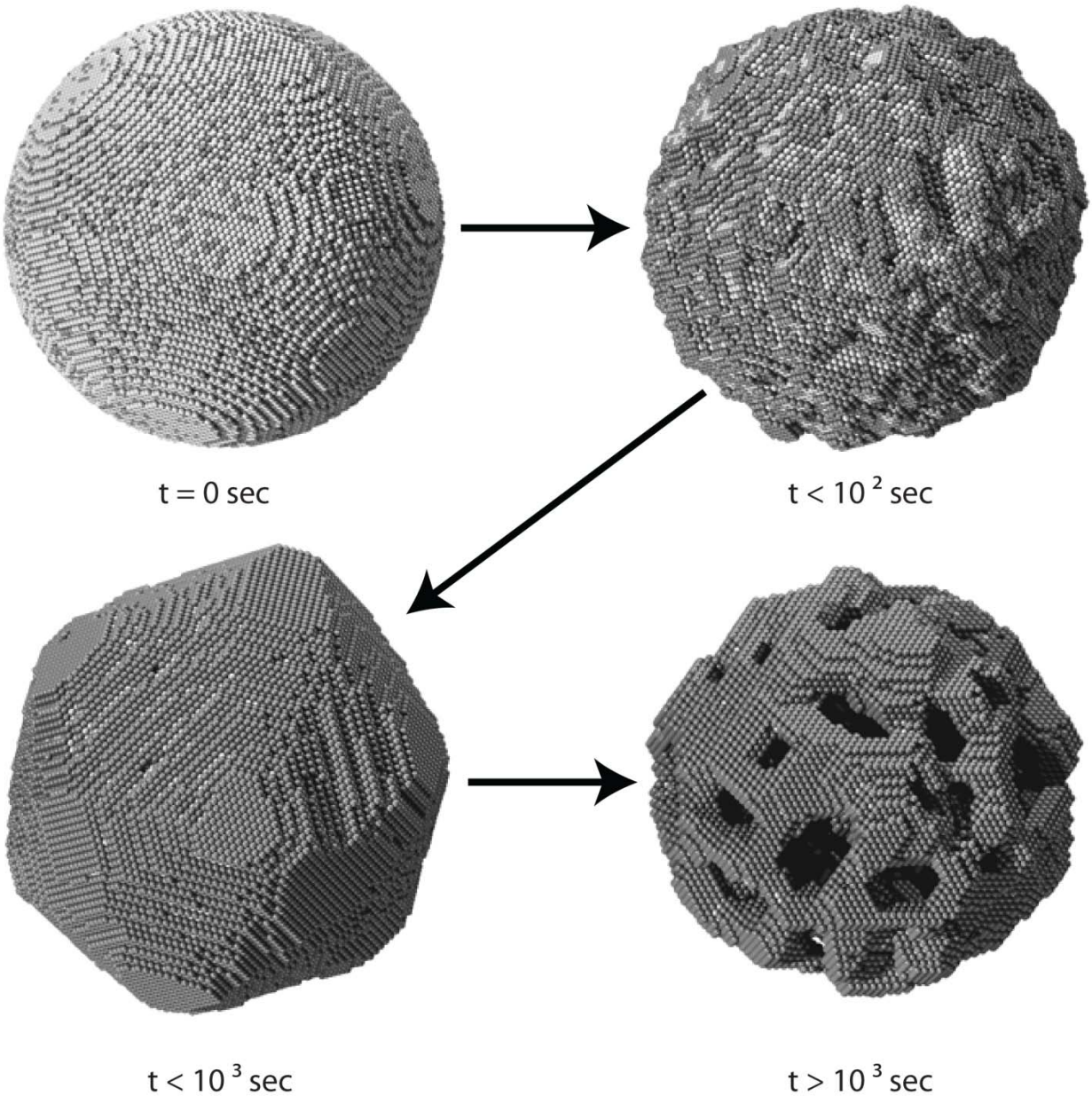

Figure 1. Time evolution of a simulated Ag-Au (white spheres: Ag; dark spheres: Au) nanoparticle (r = 30, 75 at. % Ag) under constant potential ($\phi = 0.98$eV). Initially the surface is Ag rich; it is easily stripped off and the surface roughens. The remaining Au atoms quickly form a passivating monolayer and a pseudo-equilibrated Wulff shape; eventually, a long-lived surface fluctuation reveals a percolating network of silver atoms in the bulk that dissolves to form a nanoporous nanoparticle.

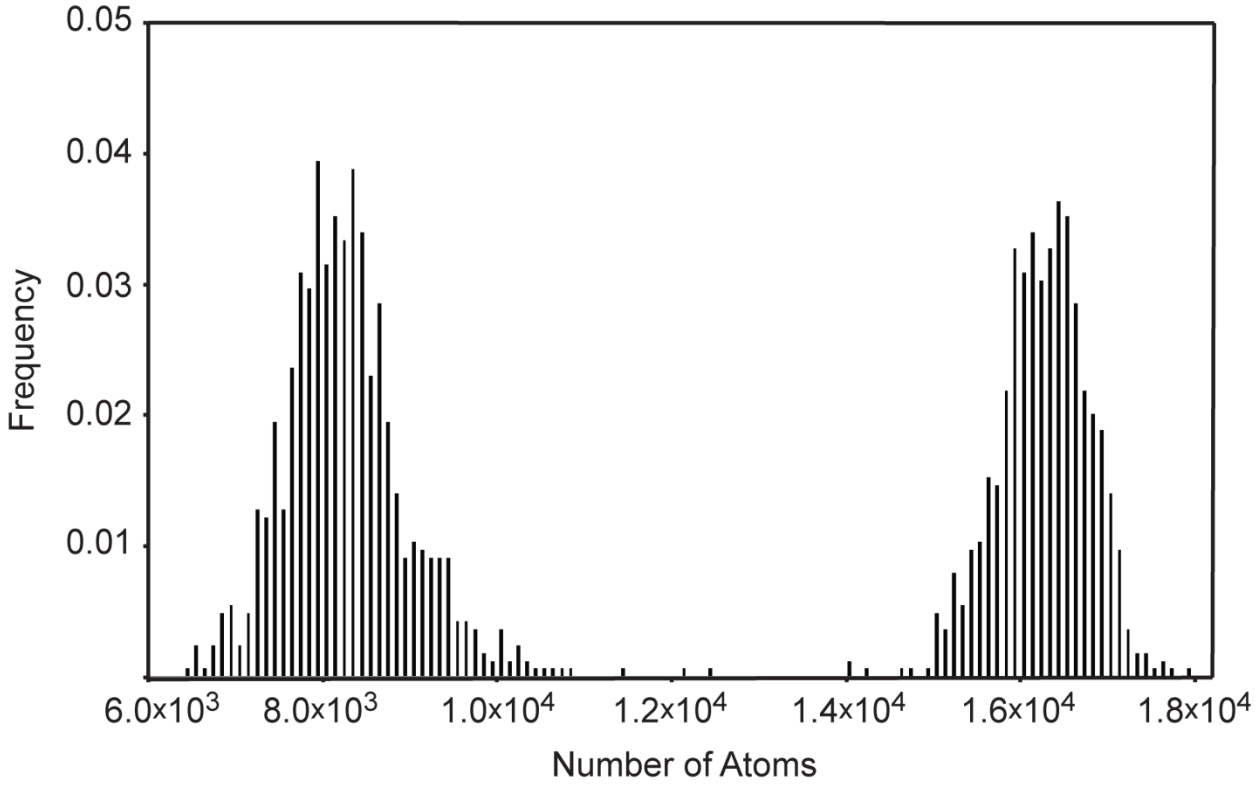

Figure 2. Histogram data of 2000 runs of a r = 18 particle, 85 at. % Ag, under constant dissolution potential $\phi = 0.975$ eV. The Gaussian at smaller number of atoms corresponds to dealloyed and porous nanoparticles while the Gaussian at larger number of atoms corresponds to passivated, but non-porous nanoparticles. The initial number of atoms for this particle radius was approximately 3.7×10^4.

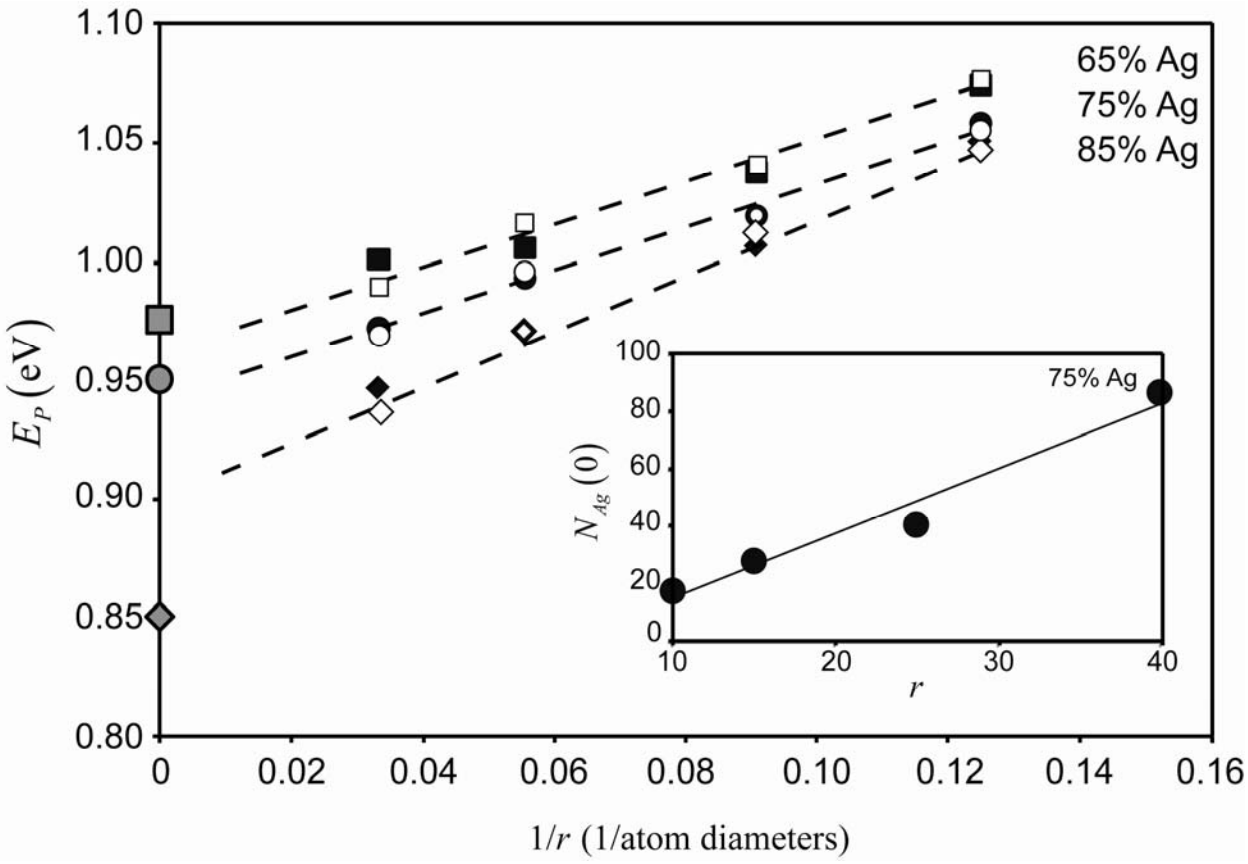

Figure 3. Simulation and model data for the potential for porosity evolution E_P versus of $1/r$. (closed symbols) measured simulation values (symbols at $1/r = 0$ correspond to values of the critical potential reported in [15]); (open symbols) predicted values of E_P using the model, Eq. (2); (grey symbols) simulation values for the critical potential for bulk porosity evolution (from Ref. []). Linear fit of the predicted values of E_P using Eq. (2) (dashed lines), shows an approximate $1/r$ dependence, and also shows that E_P generally sits at a potential higher than the bulk critical potential. (inset): the number of silver atoms in 9-coordinated sites $N_{\mathrm{Ag}}(0)$ as a function of radius for a 75 at. % particles.

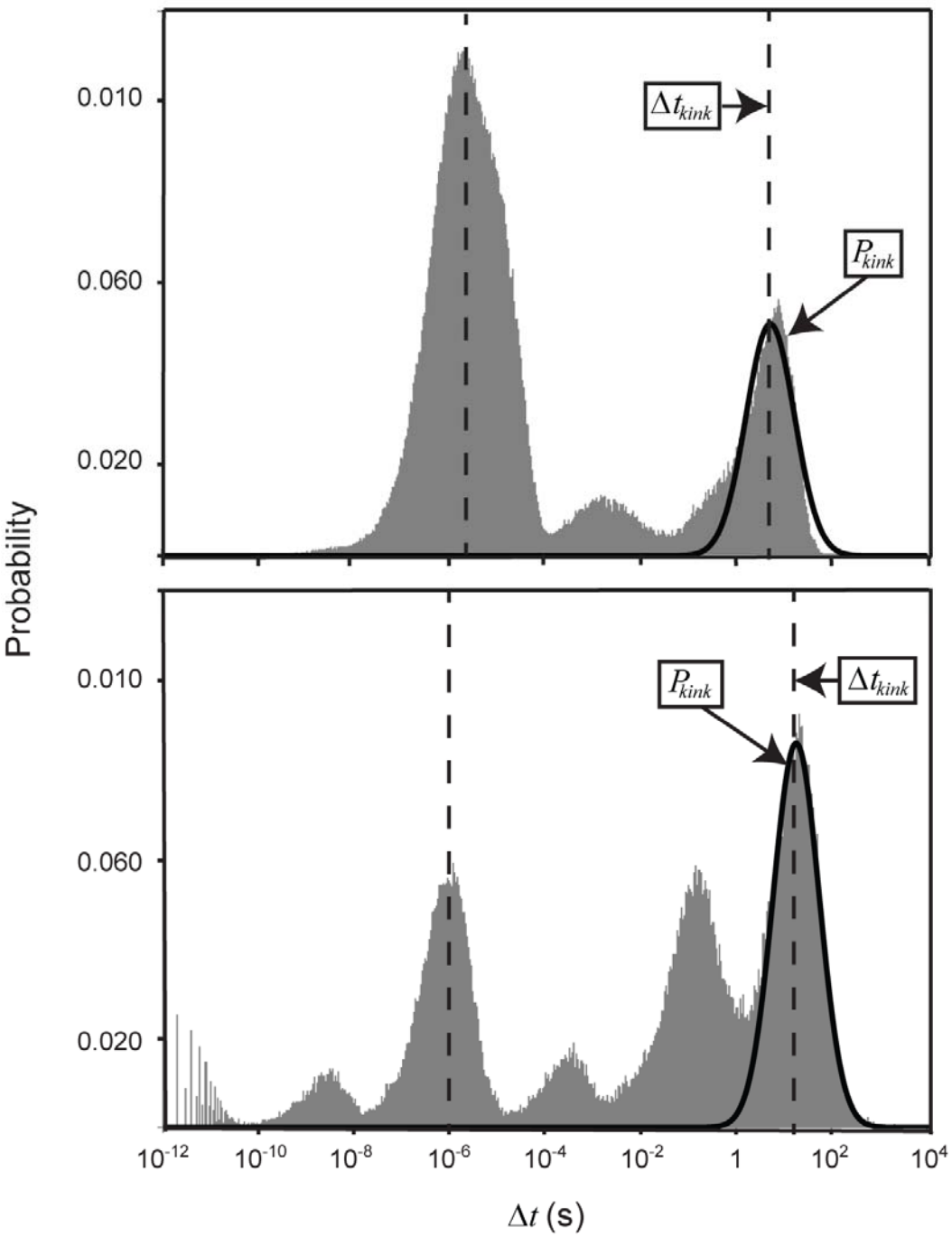

Figure 4: Surface fluctuation lifetime data for r = 8 particles (top) and r = 30 particles (bottom). The time interval Δt is the lifetime of silver atoms exposed as 9-coordinated terrace sites. By inspection, the peak at ~10^{-6} sec. corresponds to surface fluctuations associated with adatom motion (i.e., an adatom diffusing over a silver atom embedded in a (111)-oriented terrace), and the peak at ~10 sec. corresponds to fluctuations at kink sites exposing 9-coordinated silver atoms. We set Δt_{kink} to the center of this latter peak, and the area under the kink distribution to P_{kink}.